**THE EUROPEAN
PHYSICAL JOURNAL C**

Confronting models of cosmic ray interactions with particle physics at LHC energies

M.T. Dova[a], S. Ferrari

IFLP (CONICET-UNLP), Dpto. de Física, Universidad Nacional de La Plata, C.C.67 – 1900, La Plata, Argentina

Abstract. Inelastic pp collisions are dominated by soft (low momentum transfer) physics, to which perturbative QCD cannot be fully applied. A deep understanding of both soft and semi-hard processes is crucial for predictions of minimum bias and underlying events of the pp large hadron collider (LHC) now coming on line. Moreover, the interaction of cosmic ray particles entering in the atmosphere is extremely sensitive to these soft processes and consequently cannot be formulated from first principles. Because of this, air shower analyses strongly rely on hadronic interaction models, which extrapolate collider data by several orders of magnitude. A comparative study of Monte Carlo simulations of pp collisions (at the LHC center-of-mass energy $\simeq 14$ TeV) using the most popular hadronic interaction models for ultrahigh energy cosmic ray (SIBYLL and QGSJET) and for collider physics (the PYTHIA multiparton model) is presented. The most relevant distributions are studied including the observables from diffractive events with the aim of discriminating between the different models.

PACS. 13.85.-t; 96.40.-z

1 Introduction

Particle colliders and ultrahigh energy cosmic ray (UHECR) experiments today present the best scenarios to test the deep structure of matter and the interactions of its fundamental constituents at the frontier of energy. To this end, detailed modeling of the underlying physics, based on simulation programs also known as event generators, are required. These models are very important tools to define experimental and analysis strategies, to test new theoretical ideas and to design new experiments.

From the perspective of particle physics, UHECR interactions are orders of magnitude beyond what can be achieved in current (and future) terrestrial collider experiments and may open a window to energy and kinematic regions previously left unexplored in the study of fundamental interactions. The Pierre Auger Collaboration, exploiting the potential of the hybrid design of the observatory (ground based and fluorescence detectors), has developed a method to obtain the energy spectrum, which does not rely on detailed numerical simulations extrapolated from experimental knowledge of man-made accelerators to the highest cosmic ray energies [1, 2]. The hybrid detection provides a way to inter-calibrate the subsystems and to control systematic uncertainties [3]. This new approach to the derivation of the cosmic ray spectrum will allow one to constrain, although in an indirect manner,

a e-mail: Maria.Teresa.Dova@cern.ch

interaction models at energies and phase space regions that complement those of collider experiments. For the case of a primary composition determination, however, the UHECR data are interpreted in all cases using Monte Carlo simulations [4–8].

The large hadron collider (LHC) [9], currently under construction at CERN, will provide pp collisions at the unprecedented center-of-mass energy of $\sqrt{s} = 14$ TeV and a luminosity of $\mathcal{L} = 10^{34}$ cm^{-2}s^{-1}. It will also provide heavy ion collisions at a center-of-mass energy of about 1000 TeV. Good descriptions of both hard and soft processes in event generators at LHC energies are very important to understand the underlying events associated with high transverse momentum (p_T) jets or leptons as well as minimum bias events. These events will be responsible for most of the radiation background expected at LHC experiments, and hence it is essential to study detector damages, triggering systems, detector counting rates, etc. Minimum bias events are worthy of scientific study as they provide good insight into the internal structure of protons. In addition, dedicated runs of the LHC with lower luminosity ($\mathcal{L} = 10^{28}$ cm^{-2}s^{-1}) and specially tuned beam optics are planned, in order to study diffractive events. Both ATLAS [10] and CMS [11] experiments are planning to implement additional detectors to cover the forward diffractive regions with tracking and/or calorimetry [12–14]. Recently, a new experiment to study very forward particle emission in the LHC collider, LHCf, has been approved. The experimental results of LHCf will be able to provide

the production spectrum of secondary particles in the very forward region, allowing one to constrain the Monte Carlo codes [15]. Moreover, novel aspects of diffraction studies are included in the physical case of forward proton tagging at 420 m at the LHC [16]. A study of diffraction must use detectors with excellent forward acceptance to allow for a comparison with cosmic ray data. A good review of diffractive physics can be found in [17], while [18–23] focus on future studies at LHC.

In this paper we present a comparative study between the two most frequently applied models for the simulation of extensive air showers of the cosmic rays, namely SIBYLL [24] and QGSJET [25], with a multi-purpose Monte Carlo package: PYTHIA [26], tuned for use in LHC experiments. The paper is organized as follows: In Sect. 2 the main features of the models used in the Monte Carlo generators for pp collisions with emphasis on the most distinctive differences among them are presented. The method and the results from Monte Carlo studies at LHC center-of-mass energy with the aim of discriminating between the different models are described in Sect. 3. In the first part of this section, predictions for the most relevant distributions in studies of both collider and UHECR data are discussed. In the second part a comparative analysis of the signatures from diffractive events is presented. Final comments and conclusions are given in Sect. 4.

2 Models for hadronic collisions

Although electromagnetic and weak interactions are well understood, this is not the case for hadron production in collisions of nucleons, pions and kaons with light nuclei, where the lack of experimental data lead to limitations in many UHECR and accelerator applications [6, 27]. This is mainly because precise calculations of perturbative quantum chromo-dynamics (pQCD) are only possible for processes with large momentum transfer, also known as "hard" interactions, which constitute only a minute fraction of the overall reaction rate. In hadron–hadron interactions it is customary to distinguish between elastic and inelastic processes, and these latter are split into diffractive (including single and double diffraction) and non-diffractive ones (usually called minimum bias events). To be precise, low-p_T ("soft") processes, for which pQCD cannot be fully applied and phenomenological models are used, play a dominant role in the non-diffractive component.

Current models of high energy hadron collisions typically rely on the pQCD formalism in the description of high-p_T scattering, while treating the low-p_T ones in a simplified phenomenological approach. At the LHC, the description of the new physics processes to be studied are mostly controlled by pQCD. Some efforts have been made to investigate the models used by the most popular collider event generators, like PYTHIA, to describe "soft" interactions in hadron–hadron collisions with the aim of predicting minimum bias and the underlying event levels of particle production at the LHC [28–33]. These studies re-

sulted in a tuning of PYTHIA, based on comparisons of the experimental data, that is used in this paper.

The pQCD inclusive cross section of production of parton jets pairs with transverse momenta larger than some cutoff $Q_{\min}^2$ is given by

$$\sigma_{\text{QCD}}(s, p_T^{\text{cutoff}}) = \sum_{i,j} \int \frac{\mathrm{d}x_1}{x_1} \int \frac{\mathrm{d}x_2}{x_2} \int_{Q_{\min}^2}^{\hat{s}/2} \mathrm{d}|\hat{t}| \frac{\mathrm{d}\hat{\sigma}_{ij}}{\mathrm{d}|\hat{t}|}$$
$$\times x_1 f_i\left(x_1, |\hat{t}|\right) x_2 f_j(x_2, |\hat{t}|), \qquad (1)$$

where x_1 and x_2 are the fractions of the momenta of the parent hadrons carried by the partons that collide, $\mathrm{d}\hat{\sigma}_{ij}/\mathrm{d}|\hat{t}|$ is the cross section for scattering of partons of types i and j according to elementary QCD diagrams, f_i and f_j are parton distribution functions (PDFs), $\hat{s} = x_1 x_2 s$ and $-\hat{t} = \hat{s}(1 - \cos \vartheta^*)/2 = Q^2$ are the Mandelstam variables for this parton–parton process, and the sum is over all parton species.

In the UHECR field, the required information to model the interaction of the primary particle entering in the atmosphere appears to be extremely sensitive to the underlying "soft" non-perturbative hadronic process [34]. Working along these lines, there are three event generators: SIBYLL [24], QGSJET [25] and DPMJET [35]. These are tailored specifically for the simulation of hadronic interactions up to the highest cosmic ray energies.

The most frequently used high energy hadronic models in the study of UHECRs are QGSJET and SIBYLL. In these codes, the low p_T interactions are modeled by the exchange of pomerons. Regge singularities are used to determine the momentum distribution functions of the various sets of constituents, valence and sea quarks. QGSJET and SIBYLL share the eikonal model and assume unitarized cross sections and a real eikonal function sum of soft and hard contributions:

$$\sigma_{\text{inel}} = \int \mathrm{d}^2\mathbf{b} \left(1 - \exp\left\{-2\chi_s(s, \mathbf{b}) - 2\chi_h(s, \mathbf{b})\right\}\right). \quad (2)$$

At high energies the hard eikonal is dominant:

$$\chi_h = \frac{1}{2}\sigma_{\text{QCD}}(s, p_T^{\text{cutoff}})A(s, \mathbf{b}), \qquad (3)$$

where the normalized profile function $A(s, \mathbf{b})$ describes the distribution of partons in the plane transverse to the collision axis. QGSJET and SIBYLL make different assumptions on the profile function, which determines the inelastic cross section and its energy dependence.

QGSJET assumes a Gaussian profile distribution and its theory is formulated entirely in terms of pomeron exchanges. The basic idea is to replace the soft pomeron by a so-called semi-hard pomeron, defined to be an ordinary soft pomeron with the middle piece replaced by a QCD parton ladder. Thus, minijets will emerge as a part of the semi-hard pomeron, which is itself the controlling mechanism for the whole interaction.

In SIBYLL the profile function is based on the Fourier transform of the electromagnetic form factor, and it is an energy-independent exponential. The underlying idea behind SIBYLL is that the increase in the cross section is

driven by the production of minijets. The probability distribution for obtaining N jet pairs (with $p_\mathrm{T}^\mathrm{jet} > p_\mathrm{T}^\mathrm{min}$, $p_\mathrm{T}^\mathrm{min}$ being a sharp threshold on the transverse momentum below which hard interactions are neglected) in a collision at energy $\sqrt{s}$ is computed regarding elastic pp or $p\bar{p}$ scattering as a diffractive shadow scattering associated with inelastic processes. The algorithms are tuned to reproduce the central and fragmentation regions data up to $p\bar{p}$ collider energies, and with no further adjustments they are extrapolated by several orders of magnitude.

A general update of QGSJET has recently been presented, where the key improvement is connected to taking into account non-linear interaction effects in individual hadronic collisions [36]. Additionally, a more reliable low mass diffraction treatment has been used and all model parameters have been re-calibrated using a wider set of accelerator data. This results in a new model, QGSJET-II. Non-linear screening corrections appear to be correlated with corresponding parton densities and become larger at higher energies, and smaller impact parameters, resulting in the saturation of the PDFs at the scale Q_min^2 and in a considerable reduction of "soft" particle production.

In the case of PYTHIA, perturbative QCD is used, extending it to the case of low p_T. pQCD is divergent for $p_\mathrm{T} \to 0$; PYTHIA avoids the divergence using two different scenarios. The "simple scenario" consists in fixing a minimum value of $p_\mathrm{T}^\mathrm{min}$, below which the cross section is defined as null, and it can be interpreted as the inverse of some color screening length in the hadron. This is equivalent to setting a maximum impact parameter b_max, above which there is no more interaction. In the so-called "complex scenario" the regulating parameter p_T0 is introduced, below which the cross sections are dumped. Different models of matter distribution in the hadron are considered: uniform, simple Gaussian and double Gaussian.

The transition process from asymptotically free partons to color-neutral hadrons is described in all codes by string fragmentation models [38].

In summary, there are differences between the models for hadronic collisions in the existing event generators that will emerge in the Monte Carlo study presented in the rest of this paper.

3 Description of the method and Monte Carlo studies

For analyzing the differences between the models, we have generated samples of 10^4 pp collisions at the LHC center-of-mass energy for each event generator model: QGSJET-II [36], QGSJET-01 [39], SIBYLL 2.1 [40] and PYTHIA 6.205 [26]. All calculations contain a mixture of diffractive and non-diffractive events according to the model used. All secondary particles were registered without any energy cut.

In the case of PYTHIA, the "complex scenario" was chosen, with a double Gaussian distribution of matter inside the hadron. The default values of some parameters were modified according to the results of [28–33], where

the optimal values were obtained from a tuned PYTHIA, using events from different experiments. In Table 1 both default and tuned values of PYTHIA as used in this paper are presented: here MSTP(81) refers to the master switch for multiple interactions, MSTP(82) = 4 selects a hadronic matter overlap consistent with a given double Gaussian matter distribution and a continuous turn-off of the cross section at $p_\mathrm{T0} = \mathrm{PARP}(82)$. This double Gaussian matter distribution is regulated by the following parameters: a core PARP(84) of the main radius containing a fraction PARP(83) of the total hadronic matter. The value of the parameter MSTP(2) gives the kind of calculation of α_S at a hard interaction, and if the value is 1, then we have first-order running of α_S. (Here α_S is the strong coupling constant.)

3.1 General features

To help our understanding of the differences of the models currently used in the study of UHECRs, when extrapolated from collider data to higher energies and to small angle processes, it is important to compare those variables that drive the development of air showers, i.e., the multiplicity of produced secondary particles and the inelasticity (the relative energy loss of leading secondaries).

Multiplicity distributions of charged secondaries (N_ch) produced in each collision are shown in Fig. 1. Table 2 shows the average number of secondaries for each model. Besides the mean values, the standard deviations for the 10^4 interactions are given. The errors of the mean values ($\sigma/\sqrt{(10^4)}$) are much smaller. SIBYLL produces 60% to 65% less nucleons than the other models. This has been noticed in previous analyses at higher energies [4–6] and it is also seen at LHC energy. QGSJET-01 produces more baryons and charged pions than the other models, but this situation has changed in QGSJET-II, due to the non-linear screening corrections, which lead to a reduction of the interaction eikonal and hence of the number of elementary particle production processes [36]. This results in a reduction of particle production in QGSJET-II compared with QGSJET-01, bringing it closer to SIBYLL and in good agreement with the PYTHIA predictions. The mean charged particle multiplicity, which already shows differences between models at this energy, readily increases with rising energy as QGSJET predicts a power law-like increase of the number of secondaries, while the SIBYLL

Table 1. Values of relevant PYTHIA 6.2 parameters

| Variable	Default	Tunned
MSTP(81)	1	1
MSTP(82)	1	4
PARP(82)	2.1	1.8
PARP(83)	0.5	0.5
PARP(84)	0.2	0.5
MSTP(2)	1	1
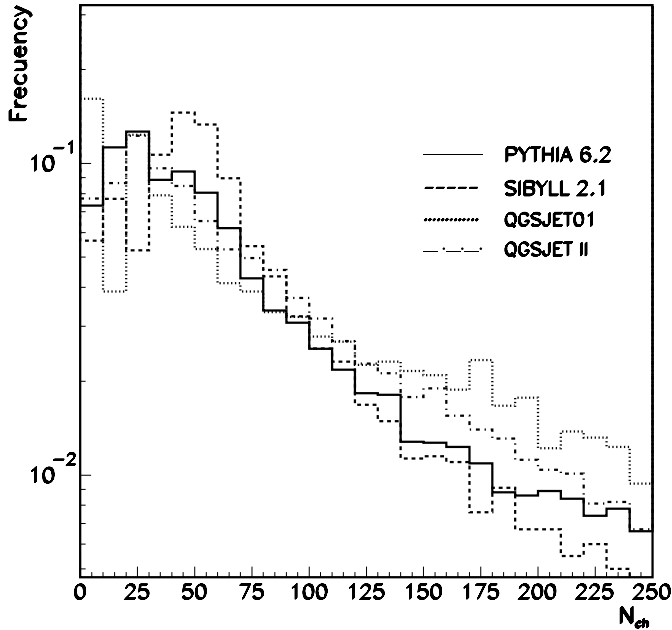
Fig. 1. Distribution of the number of charged secondaries produced in *pp* collision at LHC energy. The *solid line* corresponds to PYTHIA 6.2, the *dotted* one to QGSJET-01, the *dashed* one to SIBYLL2.1 and the *dashed-dotted* one to QGSJET-II

Table 2. Average multiplicity and inelasticity per proton–proton collision

Variable	PY 6.2	QGS 01	QGS II	SIB 2.1
p	3.8 (3.1)	3.5 (2.7)	3.9 (3.0)	2.6 (1.7)
$\overline{p}$	2.5 (3.1)	2.3 (2.2)	2.6 (2.9)	1.2 (1.6)
n	5.6 (5.9)	5.3 (5.2)	5.7 (5.7)	3.2 (3.1)
$\pi^{\pm}$	66.5 (72.1)	70.2 (68.3)	66.9 (64.5)	64.7 (60.8)
π^0	37.0 (40.4)	35.9 (34.9)	34.7 (33.7)	38.9 (37.2)
$K^{\pm}$	7.5 (8.9)	9.9 (9.9)	6.8 (6.9)	7.6 (8.1)
K_{L}	3.6 (4.5)	4.9 (5.1)	4.4 (3.7)	3.7 (4.2)
N_{charged}	80.3	85.9	80.3	76.1
N_{total}	126.5	139.3	136.1	125.7
$\langle k_{\mathrm{L}} \rangle$	0.41	0.50	0.43	0.43

multiplicity exhibits a logarithmic growth and PYTHIA follows a $\ln^2(s)$ behavior. It is worth mentioning here the results reported by the CDF collaboration favoring an energy dependence stronger than $\ln(s)$ [37].
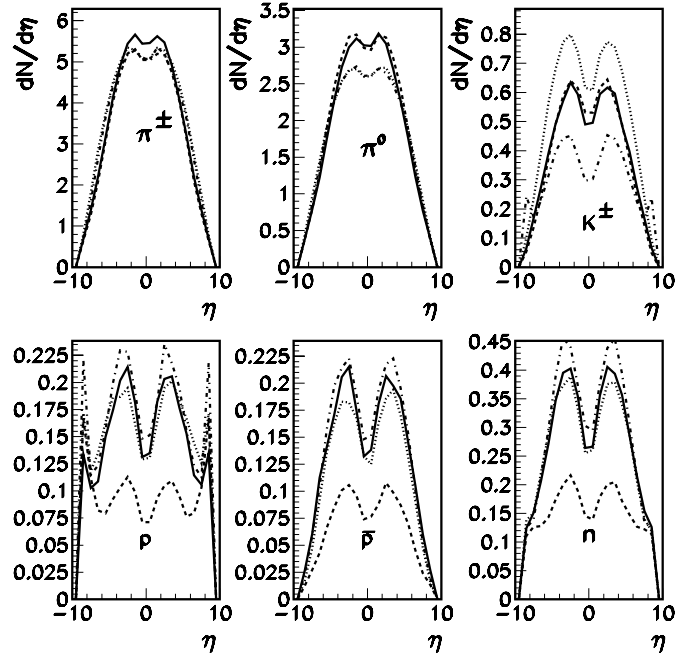
The distribution in pseudorapidity, $\eta = -\ln\tan(\theta/2)$, of charged particles for *pp* collisions at 14 TeV is presented in Fig. 2. It clearly shows that QGSJET-01 produces more secondaries than the other models in all directions but in the central region of $|\eta|$, where it is superseded by PYTHIA. This might be explained by the pure QCD treatment and the possibility of multiple interactions set in PYTHIA. It has been noticed [29] that this tuned version of PYTHIA provides the best description of the experimental data from UA5 and CDF in the central rapidity region. Above $|\eta| > 3$ PYTHIA and SIBYLL give similar
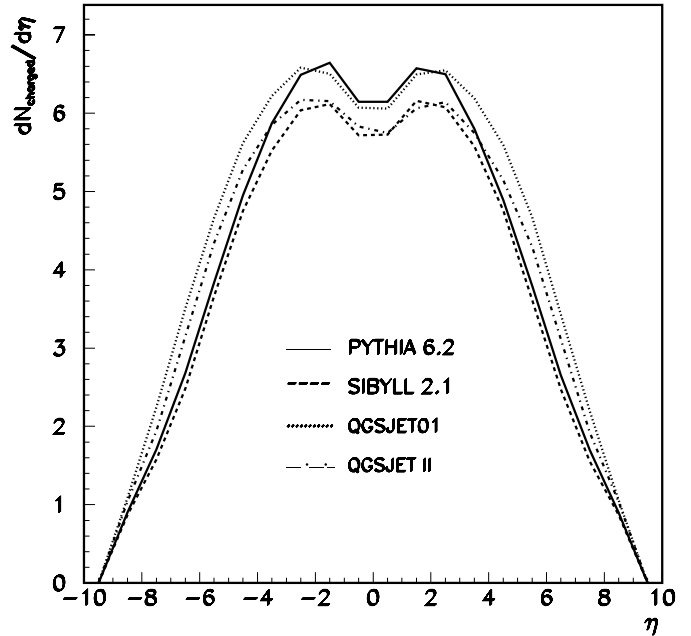

Fig. 2. Pseudorapidity distribution for charged particles

predictions, both having smaller values than the QGSJET models.

To get additional information, the pseudorapidity distributions for charged and neutral pions, kaons, protons,

Fig. 3. Pseudorapidity distribution for different types of particles. The *left-top panel* corresponds to charged pions, the *right-top* one to neutral pions, the *left-bottom* one to protons, and the *right-bottom panel* corresponds to neutrons. The *solid line* corresponds to PYTHIA 6.2 events, the *dotted* one to QGSJET-01, the *dashed* one to SIBYLL2.1 events, and the *dashed-dotted* one to QGSJET-II
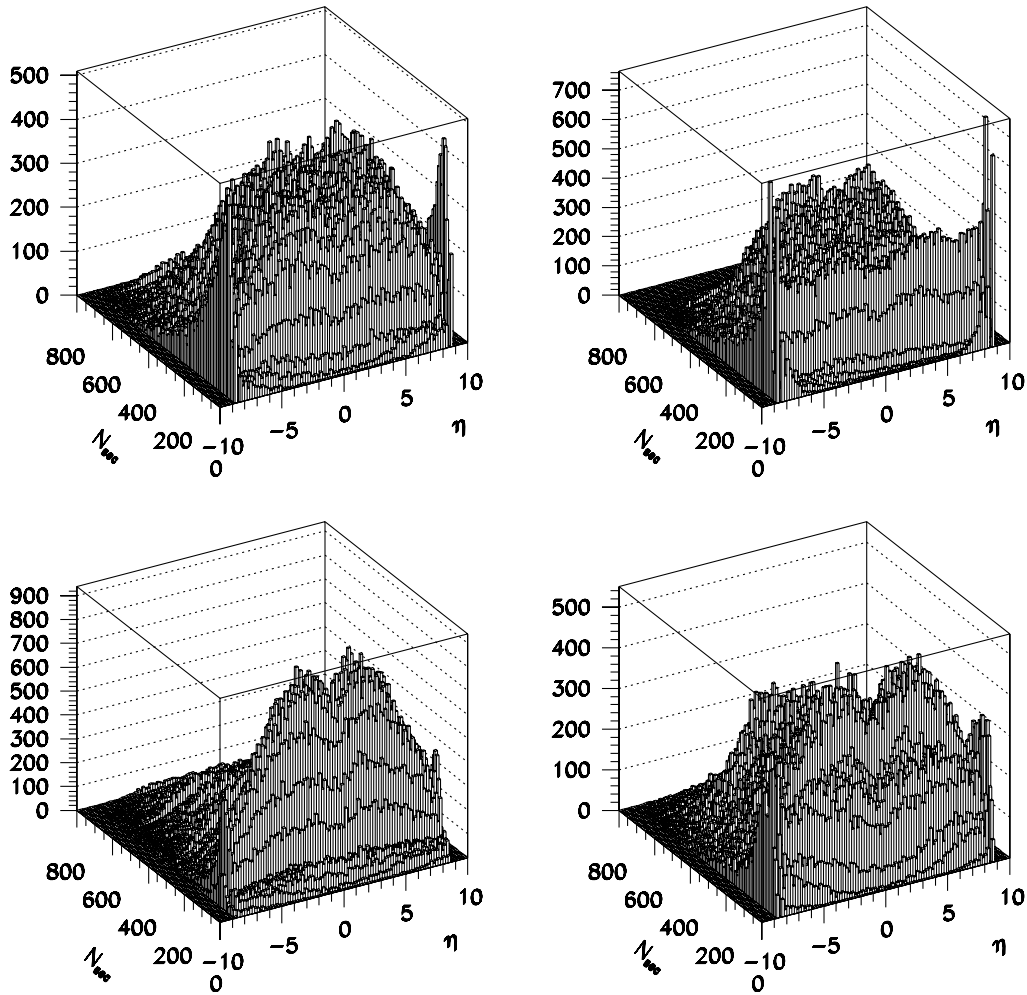
Fig. 4. Number of secondaries versus pseudorapidity 2D distribution. The *top-left panel* corresponds to QGSJET-II, the *top-right panel* corresponds to QGSJET-01, the *bottom-left panel* to SIBYLL 2.1 and the *bottom-right panel* to PYTHIA 6.2

antiprotons and neutrons are shown in Fig. 3. There are discrepancies between the models. The largest differences correspond to nucleons and antiprotons, for which, although the models predict similar shapes, SIBYLL exhibits a clear deficit at all η. For the case of kaons there is a factor of two in the predictions from the two versions of QGSJET. The peaks in the very forward and backward parts of the pseudorapidity distribution for protons correspond to diffractive events, in which one of the smashing protons keeps traveling approximately in the same direction after the collision. The shoulders in the high pseudorapidity region for neutrons have a different origin. If a neutron comes out as the fast particle, charge is being exchanged. The process, accordingly, cannot be attributed to the exchange of zero quantum numbers (i.e. to diffraction), but, for instance, has to be attributed to pion exchange. It is worth noting that the differences in the production of neutral pions influence the shower development of the secondary particles produced by the interaction of a primary cosmic ray particle in the atmosphere, which is driven by the electromagnetic component generated from the π^0.

Two-dimensional distributions of the number of secondaries, $N_{\rm sec}$, versus pseudorapidity, η, are presented in Fig. 4. The plots show in detail the large differences between QGSJET, upper panels, and SIBYLL, bottom-left panel, in the whole region of η. The two diffractive peaks in the region of low multiplicity and high pseudorapidity are well separated from the broad distribution of non-diffractive events in both versions of QGSJET and, to a lesser extent, in PYTHIA. This feature is due to the fact that QGSJET models have none or few non-diffractive events with small multiplicities, while in PYTHIA the distributions overlap and diffractive events tend to have higher multiplicities as well. For the SIBYLL model the distribution for a low number of secondaries is rather flat in all directions.

Table 3 shows the percentage frequency of the leading particle produced in the collision. In more than 50% of the collisions protons emerge as these leading particles. In SIBYLL almost 65% of the most energetic particles is a proton, while the other models give between 43% to 62%. SIBYLL and PYTHIA generate mesons as the most energetic particles in $\approx 20\%$ of the cases; however, QGSJET-01

Table 3. Most energetic secondary particle probabilities

	PYTHIA 6.2	QGSJET 01	QGSJET II	SIBYLL 2.1
proton	55.29%	43.27%	62.08%	64.62%
neutron	27.34%	18.31%	19.68%	16.51%
Σ nucleons	82.63%	61.58%	78.76%	81.13%
$\pi^{\pm}$	10.28%	20.47%	6.77%	10.72%
π^0	4.89%	9.74%	3.02%	5.85%
$K^{\pm}$	1.57%	2.40%	0.73%	1.00%
K_{L}	0.63%	0.91%	0.44%	0.57%

and QGSJET-II have larger and smaller productions of mesons as leading particles respectively with a difference of roughly a factor of 3. All models assume that the leading particle distributions scale with energy, being tuned to low energy. Certainly, measurements of hadron production in the very forward region are needed to study the leading baryon distributions, mainly because there are some theoretical models predicting that the leading particle distributions will change drastically at very high energies [27, 41].

3.2 Signatures of diffractive events

As mentioned above, in hadron–hadron interactions the inelastic processes are usually divided into diffractive and non-diffractive ones. In this section, a study of the predicted signatures from different models for diffractive hadronic interactions is presented.

A good parameter for disentangling diffractive events from pp collisions is the inelasticity, defined by

$$k_{\mathrm{L}} = 1 - \frac{E_{\mathrm{lead}}}{E_{\mathrm{P}}}, \qquad (4)$$

where E_{P} is the energy of the incident particle in the lab frame, and E_{lead} is the energy of the secondary with largest energy (the so-called leading particle). Signatures that can be used to distinguish diffractive from non-diffractive events are the low values in both inelasticity and number of secondaries [42]. In Table 2 the value of the average inelasticity for each model is shown, while the corresponding inelasticity distributions are displayed in Fig. 5. A narrow peak at low k_{L} is evident from this plot, which corresponds to elastic and single diffractive processes. For non-diffractive events, the available energy is shared among many secondaries leading to a rather uniform distribution in the whole range of k_{L}.

A few differences between models can be seen in the inelasticity distribution: PYTHIA has the highest diffractive peak. QGSJET-01 also presents a small peak at large k_{L} due to the large number of secondaries produced in inelastic collisions. QGSJET-II no longer has that feature. The SIBYLL and PYTHIA distributions are in general in good agreement.

Close inspection of the multiplicity for single diffractive, double diffractive and non-diffractive events using PYTHIA indicates that cutting at a multiplicity below 40,
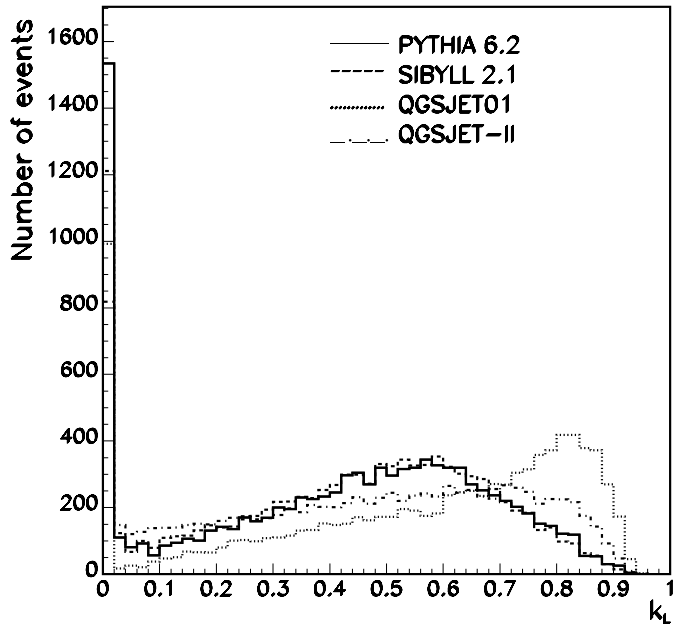
Fig. 5. Inelasticity ($k_{\mathrm{L}} = 1 - \frac{E_{\mathrm{lead}}}{E_{\mathrm{P}}}$) distribution. The *solid line* corresponds to PYTHIA 6.2, the *dotted line* to QGSJET-01, the *dashed line* to SIBYLL 2.1 and the *dashed-dotted* one to QGSJET-II

the diffractive events largely dominate the sample. However, a cut in low inelasticity ($k_{\mathrm{L}} < 0.04$) leaves an even more pure diffractive sample. We will then label as "diffractive" events the ones with inelasticity $k_{\mathrm{L}} < 0.04$. In Fig. 6 the distribution of charged particles, N_{ch}, for $k_{\mathrm{L}} < 0.04$ is presented. Both QGSJET-01 and SIBYLL distributions barely go further than 40 secondaries, while QGSJET-II and PYTHIA extend up to 60 secondaries. Figure 7 shows particle densities distributed in pseudorapidity space for "diffractive" events. There are large divergences between PYTHIA and SIBYLL in the predictions of the particle multiplicity in the whole region of η. PYTHIA predicts a density roughly 80% greater than SIBYLL. QGSJET-01 shows a rather flat distribution at intermediate values between PYTHIA and SIBYLL, while the new version, QGSJET-II, is in good agreement with PYTHIA at $|\eta| < 4$ and presents smaller values at $|\eta| > 4$. It is worth mentioning here that the cuts $k_{\mathrm{L}} < 0.04$ and $N_{\mathrm{sec}} < 40$ in the PYTHIA sample allow for selection of a pure sample of single diffractive events.
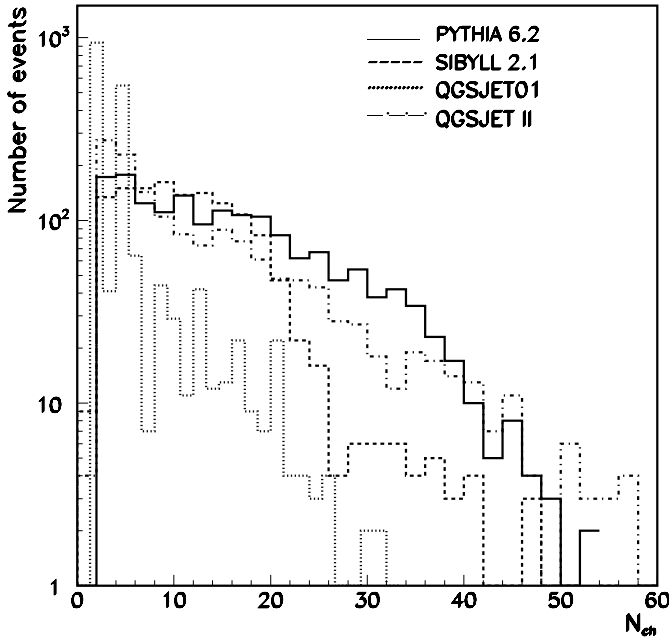
Fig. 6. Distribution of the number of secondaries for events with low inelasticity ($k_L \leq 0.04$)
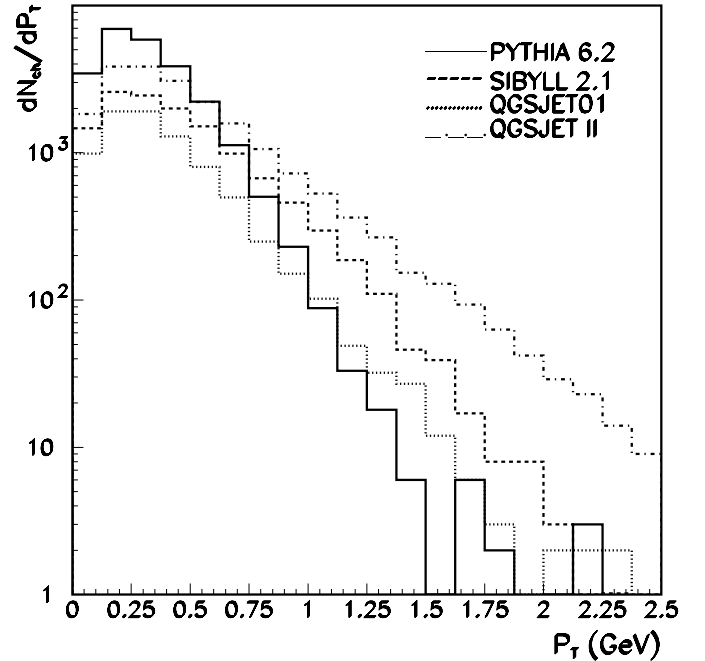

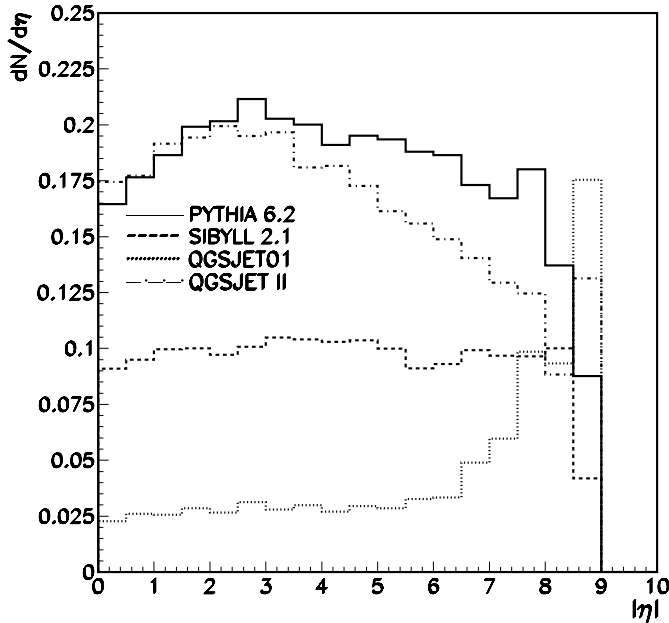**Fig. 8.** p_T distribution for the selected "diffractive" events

Fig. 7. Pseudorapidity distribution for the selected "diffractive" events

The detection capabilities for the transverse momentum, p_T, at ATLAS and CMS with a good resolution will be limited to particles with $p_T > 0.5\,\mathrm{GeV}$ [10, 11], where for the labeled "diffractive" events QGSJET-II and PYTHIA show the largest difference. This is evident in Fig. 8, where the p_T distribution of events in the central region ($|\eta| < 5$) is shown. At low momenta $\mathrm{d}N_{ch}/\mathrm{d}p_T$ is greater for PYTHIA, but as p_T increases densities for the other models become greater with a difference of an

order of magnitude at $p_T > 1.5$ for the case of QGSJET-II, as PYTHIA does not create diffractive events with high transverse momentum.

Figure 9 shows 2D distributions of the number of secondaries in the events labeled "diffractive" versus pseudorapidity. Again, it is evident that the distributions generated by SIBYLL are fundamentally different from the ones from QGSJETs and PYTHIA. This is certainly due to the phenomenological description of the diffractive events in SIBYLL [24]. QGSJET-01 and QGSJET-II predict a large fraction of events with a low number of secondaries in the region of high pseudorapidity. Clearly, the better treatment of diffraction for the case of QGSJET-II with its parameters tuned using accelerator data results in diffractive peaks much lower than in QGSJET-01, but still larger compared with PYTHIA data.

4 Conclusions

The two most widely used high energy hadronic interaction models for the study of cosmic rays, SIBYLL and QGSJET, and the most popular simulation program for collider experiments, PYTHIA, have been compared at LHC center-of-mass energy. These codes, using different theoretical models involving many variables, have different predictions for the most important observables, such as particle multiplicities, distribution of particles in pseudorapidity space and transverse momentum distribution, allowing one to investigate and improve the theoretical predictions of hadron–hadron interactions at this energy.

The discrepancies observed in the pseudorapidity distributions for different types of particle, in particular in the
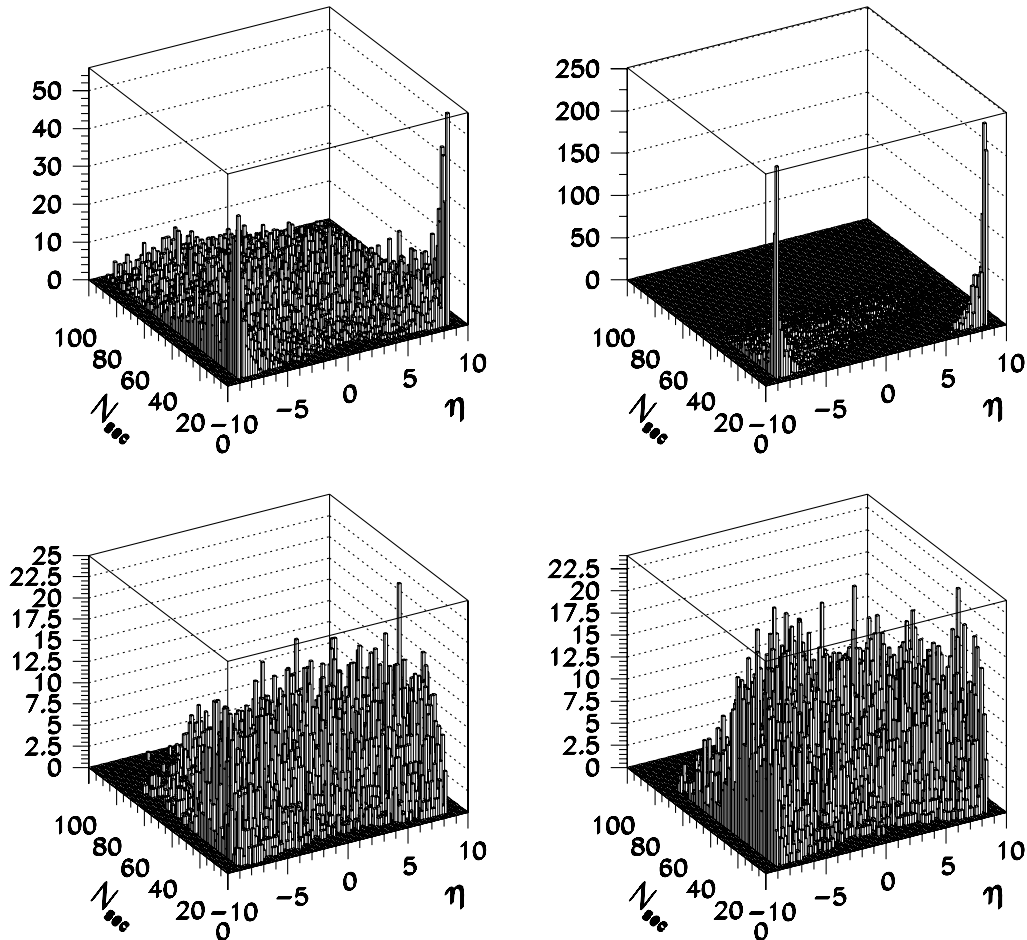
Fig. 9. Multiplicity versus pseudorapidity 2D distribution for low inelasticity ($k_L \leq 0.04$) events. The *top-left panel* corresponds to QGSJET-II, the *top-right panel* corresponds to QGSJET-01, the *bottom-left panel* to SIBYLL 2.1 and the *bottom-right panel* to PYTHIA 6.2

acceptance region of LHC experiments would allow one to perform a combined analysis to constrain the models, using the large minimum bias events statistics that will be collected in the very first LHC operation. The predictions for the 2D distributions of particle multiplicity versus pseudorapidity will also help in deciding on the best theoretical model.

Measurements of hadron production with the forward detectors attached to LHC experiments are very important for a better understanding of the simulations that model soft hadronic interactions at high energies. The analysis of the percentage frequency of the leading particle produced in the collision indicates differences up to a factor of 2 for meson production.

A selection of events from pp collisions at $\sqrt{s} = 14$ TeV with small inelasticity ($k_L < 0.04$) and a low number of secondaries allows one to pick diffractive events for a comparative study of the various models. The analysis of particle densities in pseudorapidity space indicates good agreement of predictions using PYTHIA and QGSJET-II and a clear deficit of particle densities using SIBYLL and to a lesser extent QGSJET-01. The p_T distributions in the central pseudorapidity region clearly indi-

cate that the SYBYLL and QGSJET models create up to an order of magnitude more particles with large p_T than PYTHIA. A comparison with experimental data will provide strong constraints in modeling diffractive physics.

The lack of suitable accelerator data is the dominant source of systematic uncertainties in the analysis of the extensive air shower data. At the same time, the analyses of minimum bias events at LHC are very important for understanding the underlying events and commissioning studies for LHC detectors. Certainly, the discrepancies in the models discussed in this paper will naturally be reduced with the large statistics of interesting data at a completely new energy frontier for terrestrial colliders, such as LHC, and cosmic ray experiments, such as the Pierre Auger Observatory.

References

1. P. Sommers, Comments Nucl. Part. Phys. A **2**, 261 (2002)
2. J.W. Cronin et al., FERMILAB-PROPOSAL-0881, Jul 1995, p. 18
3. Auger Collaboration, M. Kleifges, Nucl. Instrum. Methods A **518**, 180 (2004)
4. L.A. Anchordoqui, M.T. Dova, L.N. Epele, S.J. Sciutto, Phys. Rev. D **59**, 094 003 (1999) [hep-ph/9810384]
5. L. Anchordoqui, M.T. Dova, A. Mariazzi, T. McCauley, T. Paul, S. Reucroft, J. Swain, Ann. Phys. **314**, 145 (2004) [hep-ph/0407020]
6. R. Knapp, D. Heck, S.J. Sciutto, M.T. Dova, M. Risse, Astropart. Phys. **19**, 77 (2003)
7. M. Nagano, D. Heck, K. Shinozoki, N. Inoue, J. Knapp, Astropart. Phys. **13**, 277 (2000)
8. S.C. Corbato et al., Nucl. Phys. Proc. Suppl. B **28**, 36 (1992)
9. LHC Study Group 1995 The large hadron collider conceptual design, CERN/AC/95-05
10. ATLAS Collaboration, Detector and Physics Performance TDR, CERN-LHCC/99-14, 1999
11. CMS Collaboration, Technical Design Report, CERN-LHCC 2006-21
12. G. Matthiae, Nucl. Phys. Proc. Suppl. A **99**, 281 (2001)
13. TOTEM Collaboration, TOTEM: Technical Design Report, CERN-LHCC-1997-049, CERN-LHCC-1999-007, CERN-LHCC-2004-002, CERN-LHCC-2004-020
14. M. Rijssenbeek, Nucl. Phys. Proc. Suppl. **122**, 459 (2003)
15. O. Adriani et al., CERN-LHCC-2006-004
16. M. Albrow et al., CERN-LHCC-2005-025
17. E. Pedrazzi, Lectures given at 6th Workshop on Hadron Physics, Florianopolis, Santa Catarina, Brazil, 16–21 March, 1998 [hep-ph/9809454]
18. A. de Roeck, Acta Phys. Pol. B **33**, 3591 (2002)
19. CDF Collaboration, M. Gallinaro, hep-ph/0410232
20. S.M. Troshin, N.E. Tyurin, prepared for 15th International Workshop on High-Energy Physics and Quantum Field Theory (QFTHEP 2000), Tver, Russia, 14–20 September 2000
21. L. Frankfurt, M. Strikman, C. Weiss, M. Zhalov, Czech. J. Phys. B **55**, 675 (2005) [hep-ph/0412260]
22. V.A. Khoze, A.D. Martin, M.G. Ryskin, Eur. Phys. J. C **23**, 311 (2002) [hep-ph/0111078]
23. S. Tapprogge, prepared for 26th Johns Hopkins Workshop on High-Energy Reactions, from the Standard Model to String Theory, from Colliders to Cosmic Rays, Heidelberg, Germany, 1–3 August 2002
24. R.S. Fletcher, T.K. Gaisser, P. Lipari, T. Stanev, Phys. Rev. D **50**, 5710 (1994)
25. N.N. Kalmykov, S.S. Ostapchenko, A.I. Pavlov, Nucl. Phys. Proc. Suppl. B **52**, 17 (1997)
26. T. Sjöstrand, P. Edén, C. Friberg, L. Lönnblad, G. Miu, S. Mrenna, E. Norrbin, Comput. Phys. Commun. **135**, 238 (2001)
27. R. Engel, Nucl. Phys. Proc. Suppl. **151**, 437 (2006) [astro-ph/0504358]
28. A. Kupčo, ATL-PHYS-99-019 (1999)
29. A. Moraes, I. Dawson, C. Buttar, ATL-PHYS-2003-020 (2003)
30. I. Dawson, C. Buttar, A. Moraes, Czech. J. Phys. **53**, A1 (2003)
31. C.M. Buttar, D. Clements, I. Dawson, A. Moraes, Acta Phys. Pol. **35**, 433 (2004)
32. J.P. Guillaud, A. Sobol, LAPP-EXP 2004-06
33. A. Moraes, C. Buttar, I. Dawson, ATL-PHYS-PUB-2005-007
34. S.S. Ostapchenko, J. Phys. G **29**, 831 (2003)
35. J. Ranft, hep-ph/9911232
36. S. Ostapchenko, Nucl. Phys. B Proc. Suppl. **151**, 143 (2006) [hep-ph/0501093]
37. CDF Collaboration, R. Abe et al., Phys. Rev. D **41**, 2330 (1990)
38. T. Sjöstrand, Int. J. Mod. Phys. A **3**, 751 (1988)
39. D. Heck, Proc. of 27th Int. Cosmic Ray Conf. 1, p. 233, Hamburg, Germany, 2001
40. R.T. Engel, T.K. Gaisser, P. Lipari, Stanev, Proc. of 26th ICRC (Salt Lake City) 1, p. 415, 1999
41. L. Frankfurt, W. Koepf, M. Strikman, Phys. Lett. B **405**, 367 (1997)
42. R. Luna, A. Zepeda, C.A. García Canal, S.J. Sciutto, Phys. Rev. D **70**, 1140 (2004)